Density and phase equilibrium of the binary system methane + n-decane under high temperatures and pressures

Regueira Muñiz, Teresa; Pantelide, Georgia; Yan, Wei; Stenby, Erling Halfdan

Published in:
Fluid Phase Equilibria

Link to article, DOI:
10.1016/j.fluid.2016.08.004

Publication date:
2016

Document Version
Peer reviewed version

Density and phase equilibrium of the binary system methane + n-decane under high temperatures and pressures

Teresa Regueira, Georgia Pantelide, Wei Yan*, Erling H. Stenby

Center for Energy Resources Engineering (CERE), Department of Chemistry, Technical University of Denmark, DK-2800 Kgs. Lyngby, Denmark

*Corresponding author: E-mail: weya@kemi.dtu.dk; Tel.:+45 45252914; Fax: +45 45882258

Abstract

Densities of the binary system methane + n-decane have been determined through a vibrating tube densitometer from (278.15 to 463.15) K at pressures up to 140 MPa, and for methane mole fractions up to 0.8496. Negative excess volumes were found under the experimental conditions studied. Moreover isothermal compressibility values were obtained by differentiation from the Tammann-Tait correlation of the determined density values. Isobaric thermal expansion coefficients were also calculated based on differentiation from the isobaric fit of density data. We also measured the phase equilibrium of this binary system by using a variable volume cell with full visibility from (293.15 to 472.47) K for three mixtures with methane mole fractions of 0.4031, 0.6021 and 0.8496. Liquid fraction upon expansion below the saturation pressure has also been determined. Finally different equations of state were used to calculate the experimental density and excess volume data as well as the phase envelope data. No direct regression of the experimental data was involved in most of the calculation in order to provide a fair comparison of the performance of different models.

Keywords

Density, phase equilibrium, high pressure-high temperature, methane, n-decane

1. Introduction

The increasing demand in oil and gas and the decline of conventional reservoirs leads to the exploration of reservoirs in greater depths that are characterized by high pressure and high temperature (HPHT) conditions [1,2]. In order to plan and predict the production under these conditions, it is essential to accurately describe the fluid properties of the reservoir fluids, in particular their density and phase behavior. The use of well-defined hydrocarbon mixtures as an approach to model reservoir fluids is quite common [3-8] because they capture the main features and trends of the phase behavior and properties of the real reservoir fluids, whose samples are very difficult to obtain from the HPHT wells. However, data on the thermophysical properties of such mixtures is still scarce under HPHT conditions, especially for highly asymmetric ones. These data are particularly useful for evaluating the capability of the existing thermodynamic models for asymmetric systems at HPHT conditions. Although these data cannot replace PVT study of actual

reservoir fluids completely in developing better models for HPHT reservoir fluids, there is one advantage of using these data in the modeling study, namely, no reservoir fluid characterization is involved and the model evaluation is not affected by the uncertainty in the treatment of the ill-defined heptanes plus fractions in the reservoir fluids.

Among the relevant thermophysical properties, density and its derived properties like isothermal compressibility and isothermal thermal expansion coefficient have great importance. Density and isothermal compressibility are used for estimation of oil and gas resources and forecast of oil and gas production. Density is also related to other volumetric and thermodynamic properties [9]. Therefore, following a previous work [10] in which we measured the density of the binary alkane systems n-hexane + n-decane and n-hexane + n-hexadecane from (278.15 to 463.15) K and up to 60 MPa in the whole composition range, in this work, density was measured through a vibrating tube densitometer for the binary system methane + n-decane with methane mole fractions up to 0.8496 in the temperature range (278.15 to 463.15) K and up to 140 MPa. This binary system has been previously studied by Audonnet and Pádua [4] in the temperature range (298 to 393) K and pressures up to 75 MPa for five different compositions. Also, Canet et al. [11] performed density measurements for this binary system at temperatures ranging from (293.15 to 373.15) K and pressures up to 65 MPa and then extrapolated density data up to 140 MPa through a Tait-type equation. Therefore, the data reported in the present work extends the existing temperature range both to lower and higher temperatures, as well as to higher pressures.

The obtained density data were correlated in the present work as a function of temperature and pressure using a modification of the Tammann-Tait equation. Additionally, isothermal compressibility, isobaric thermal expansion coefficient and excess volumes were reported. Negative excess volumes were found in the studied (p,T,x) range. Moreover, the capabilities of four different EoSs, i.e. Soave-Redlich-Kwong (SRK) [12], Peng-Robinson (PR) [13], Perturbed Chain Statistical Associating Fluid Theory (PC-SAFT) [14], and Soave-Benedict-Webb-Rubin (S-BWR) [15] to calculate the density data as well as the excess volume were analyzed.

Besides, the knowledge of the phase behavior of hydrocarbon fluids in broad temperature and pressure conditions is crucial to understanding the fluid behavior under reservoir depletion. In fact, there are many cases in which the fundamentals of the phase behavior of reservoir fluids can be understood through the study of binary and multicomponent alkane mixtures [16]. Phase equilibrium data of the binary system methane (1) + n-decane (2) were also determined in this work at three different compositions, x_1=0.4031, x_1=0.6021 and x_1=0.8496 from (293.15 to 472.47) K. Thus, saturation pressures were visually determined using a recently installed technique consisting of a variable volume cell with full visibility. Data on this system were previously reported by Sage et al. [17] who published results at temperatures between 294 and 394 K and by Reamer et al. [18] who reported equilibrium pressures at temperatures between 310 and 510 K. Also, Rijkers et al. [7] studied the phase behavior of methane + n-decane in the temperature range from (240 to 315) K. Liquid fraction measured after expansion below the saturation pressure is also reported in this work and it was used for distinguishing between bubble and dew points for the mixture with x_1=0.8496. Finally, the phase equilibrium data were modeled using the SRK, PR, and PC-SAFT and S-BWR EoSs finding that the calculation results are poor for the mixture with high methane mole fraction (x_1=0.8496) through all the analyzed EoSs.

It should be noted that the methane/n-decane binary interaction parameters k_{ij} for SRK, PR, PC-SAFT and S-BWR were taken from Yan et al. [19] in all our density, excess volume and phase envelope calculations except for the additional discussion of k_{ij} tuning for the phase envelope of the mixture with methane mole fraction of 0.8496. The k_{ij} values were regressed from a large set of binary VLE data [19] and no experimental data from this work were used in the regression. In this sense, the modeling of the experimental data in this study is predictive. Of course, one should distinguish between the "predictive" calculations in our context and pure predictions with zero k_{ij}, the latter being used in many studies but not here. However, the influence of k_{ij} on volumetric properties is usually small and such a distinction is unimportant in the density and excess volume modeling.

2. Materials and methods

Methane was acquired from AGA, with mole purity of 99.9995%, whereas n-decane was purchased from Sigma Aldrich with mole purity ≥ 99%. N-decane was degasified by means of an ultrasonic bath (Branson 1510) prior to mixture preparation. Milli-Q water with resistivity of 18.2 MΩ·cm and n-dodecane (Sigma Aldrich mole purity ≥ 99%) were used for densitometer calibration. A summary of the provenance and purity and of the samples is presented in Table 1.

Table 1

Sample description

Chemical name	Source	Initial mole-fraction purity*	Purification method	Analysis method*
methane	AGA	0.999995	none	-
n-decane	Sigma Aldrich	0.996	none	Gas chromatography (GC)
n-dodecane	Sigma Aldrich	0.998	none	Gas chromatography (GC)

*Given by the manufacturer

Mixtures for density measurements were prepared in a high pressure cylinder that contains a piston which separates the hydraulic fluid (water) from the sample. Moreover, in the sample side there is a stainless steel sphere which is used for the homogenization of the mixture. First the sample side of the cylinder is evacuated and then the n-decane is added to the cylinder by means of a burette with a standard uncertainty of 0.01 cm^3. Afterwards methane is added gravimetrically from a high pressure cylinder by using an analytical balance Mettler Toledo PR1203, which has a standard uncertainty of 0.001g.

The mole fraction composition of the binary mixtures methane (1) + n-decane (2) studied in the densitometer were x_1=0.2272, x_1=0.4520, x_1=0.6017, x_1=0.7085 and x_1=0.8496. The phase equilibrium of this last mixture was also studied. The uncertainty of the mole fraction composition with an expanded uncertainty k=2 is $3 \cdot 10^{-4}$.

Additionally, the phase equilibrium of two more binary mixtures methane (1) + n-decane (2) was studied. These mixtures were prepared with the aid of a high pressure pump (Sanchez Technologies SDS collecting pump, VPDS45°200/1500), which pumped the needed volume of methane and n-decane into the PVT cell at constant pressure of 10 MPa. The density of both compounds had been previously determined by pumping a known volume of each compound to two evacuated cylinders at constant pressure of 10 MPa. Afterwards, the mass transferred was weighed through an analytical balance Mettler Toledo PR 1203. Density was obtained from the measured mass and volume. The measured densities along with the volume pumped to the PVT cell were used to calculate the mole fractions of the prepared mixtures, x_1= 0.4031 and x_1=0.6021. The uncertainty of the mole fraction composition for these two mixtures with an expanded uncertainty k=2 is $5 \cdot 10^{-4}$.

2.1. Experimental

Density measurements were performed through a vibrating tube densitometer DMA HPM from Anton Paar, which displays oscillation periods with seven significant figures. The schematic of the experimental setup is presented in Fig. 1.

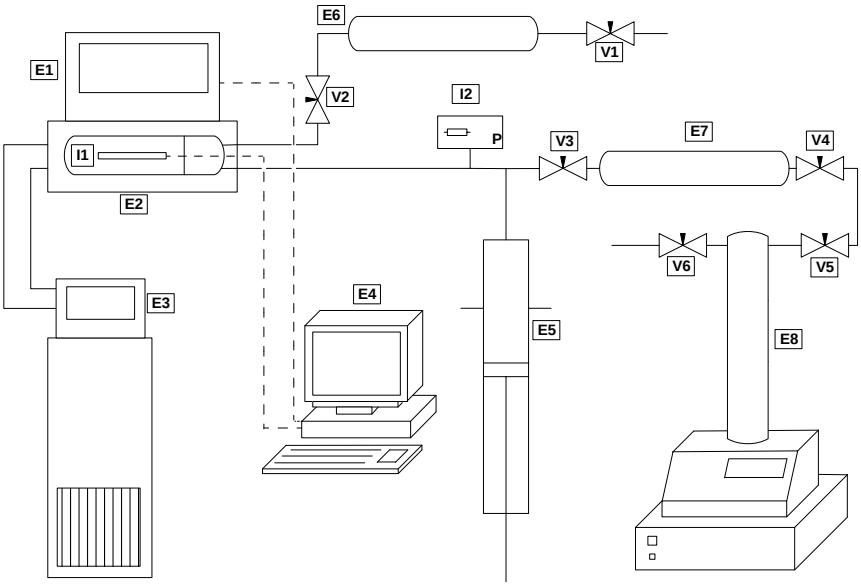

Fig. 1. Scheme of the experimental setup for density measurements. (E1) mPDS 5 unit, (E2) DMA HPM measurement cell, (E3) thermostatic bath, (E4) computer, (E5) pressure generator, (E6) buffer cylinder, (E7) injection cylinder, (E8) syringe pump, (I1) Pt100, (I2) pressure transducer, (V1-V6) high pressure valves.

The sample was prepared in the injection cylinder and transferred to the evacuated densitometer by means of an isobaric process at a pressure higher than the saturation one in order to keep the binary mixture in a homogenous single phase state. During the isobaric transfer pressure is kept constant through the syringe pump (Teledyne Isco 100 DX). Once the transfer was performed the densitometer was purged five times the volume of the system (20 cm^3) to the buffer cylinder in order to assure that composition in the measuring cell of the densitometer was the same as the one of the mixture prepared in the injection cylinder.

During density measurements the temperature was controlled through a thermostatic bath PolyScience PP07R-20-A12E which regulates temperature within ±0.005 K. The temperature was measured by means of a Pt100 inserted inside the measurement cell with a standard uncertainty of 0.02 K. As concerns pressure it was generated manually by means of a high pressure generator (HiP 37-6-30) and it was measured with a pressure transducer SIKA type P which can measure pressures up to 150 MPa with a standard uncertainty of 0.05 % FS.

As concerns the calibration of the densitometer, it was performed in the temperature range from (278.15 to 463.15)K and pressures from (0.1 to 140) MPa, following a procedure similar to that described by Comuñas et al. [20], using vacuum, Milli-Q water and n-dodecane as reference fluids. N-dodecane was the reference fluid in the temperature and pressure conditions where water is vapor, i.e. at $T \geq 373.15$ and p = 0.1 MPa and also at T = 463.15 K and p = 1 MPa. The equations used to obtain the density values from the measured oscillation periods were as follows:

For T < 373.15 K:

$$\rho(T,p) = \rho_w(T,p) + \rho_w(T,0.1\ \text{MPa})\frac{\tau^2(T,p) - \tau_w^2(T,p)}{\tau_w^2(T,0.1\,\text{MPa}) - \tau_v^2(T,0)} \quad (1)$$

where ρ_w is the density of water taken from Wagner and Pruß [21] and τ, τ_w and τ_v are the oscillation periods of the measured sample, water and vacuum, respectively.

For $T \geq$ 373.15 K and p = 0.1 MPa, as well as for T = 463.15 K and p = 1 MPa:

$$\rho(T,p) = \rho_d(T,p) + \rho_d(T,0.1\ \text{MPa})\frac{\tau^2(T,p) - \tau_d^2(T,p)}{\tau_d^2(T,0.1\,\text{MPa}) - \tau_v^2(T,0)} \quad (2)$$

where ρ_d is the density of n-dodecane taken from Lemmon and Huber [22] and τ, τ_d and τ_v are the oscillation periods of the measured sample, n-dodecane and vacuum, respectively.

Under any other conditions, i.e. T = 373.15 K and T = 423.15 K at p > 0.1 MPa, and T = 463.15 K at p > 1 MPa:

$$\rho(T,p) = \rho_w(T,p) + \rho_d(T,0.1\,\text{MPa})\frac{\tau^2(T,p) - \tau_w^2(T,p)}{\tau_d^2(T,0.1MPa) - \tau_v^2(T,0)} \quad (3)$$

where τ, τ_w, τ_d and τ_v are the oscillation periods of the measured sample, water, n-dodecane and vacuum, respectively.

The expanded (k=2) uncertainty of the density measurements has been previously reported by Segovia et al. [23]. It is considered to be $7\cdot10^{-4}$ g·cm^{-3} at T < 373.15 K, $5\cdot10^{-3}$ g·cm^{-3} at $T \geq$ 373.15 K and p = 0.1 MPa, as well as for T = 463.15 K and p = 1MPa, and $3\cdot10^{-3}$ g·cm^{-3} in other temperature and pressure conditions.

With this setup density of the binary mixtures was measured from 278.15 K to 463.15 K up to 140 MPa. The minimum pressure of the density measurements was limited by the saturation pressure of the samples.

As concerns the determination of the phase equilibrium of the binary mixtures it was performed using a PVT unit PVT 240/1500 from Sanchez Technologies with full visibility (Fig. 2). The apparatus consists of a hollow cylinder with a sapphire window at one end and a motorized piston at the other end. The maximum volume of the cell is 240 cm^3 and it can operate in the pressure range up to 150 MPa and in the temperature range up to 473.15 K.

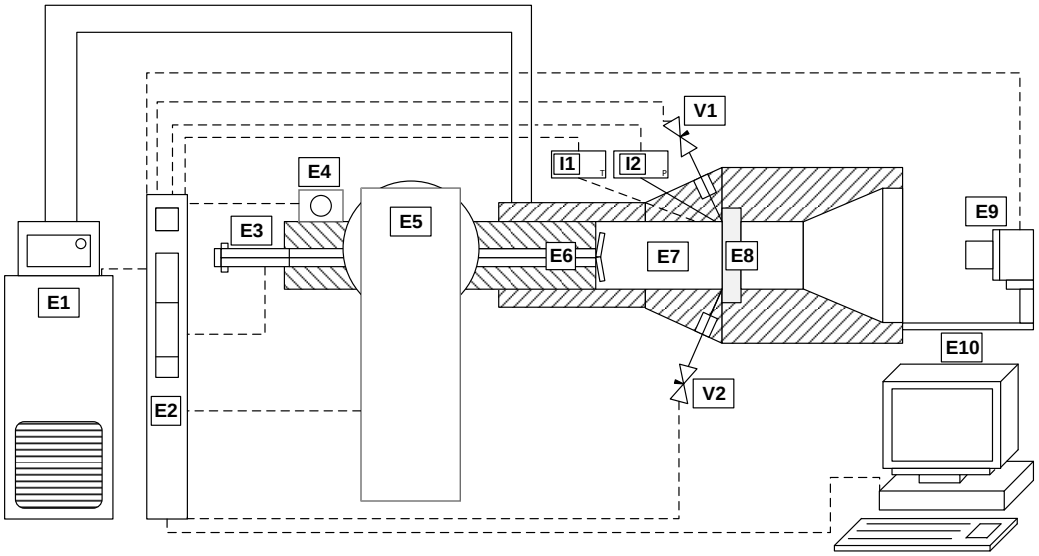

Fig. 2. Scheme of the PVT apparatus. (E1) thermostatic bath, (E2) control box, (E3) stirrer motor, (E4) piston motor, (E5) rotation system, (E6) piston with retractable blades, (E7) cell, (E8) sapphire window, (E9) video camera, (E10) computer, (I1) Pt100, (I2) pressure transducer, (V1,V2) high pressure valves.

Pressure is generated in the system through a motorized piston and it was measured by means of a pressure transducer Dynisco PT435A which was calibrated in the experimental pressure and temperature conditions against a reference pressure transducer, and thus it measured pressure with a standard uncertainty of 0.06 MPa. In the head of the piston it is attached a mechanical stirring system consisting of four retractable blades which was used to make the mixture homogeneous. The temperature is kept constant within 0.1 K by means of an electric heating system comprised of eight heating resistances installed in the body of the cell, which assures the homogeneous heating of the sample. Additionally, a circulating bath Julabo Presto A40 connected to the PVT cell was used to cool down the system and to improve the temperature stability of the cell. Temperature was measured within 0.02 K by means of a Pt100 located in the wall of the cell.

This PVT cell (Fig. 2) was operated by means of the Falcon software, whereas the visual observation of the cell during the experiments was performed using a CCD digital camera Lumenera Lw1335C, placed in front of the sapphire window, along with the Euclide software version 1.4.2. The saturation pressure was determined by visual observation by lowering the pressure at constant temperature from the single phase region. The pressure was decreased while stirring by increasing the cell volume with a constant flow rate of $8.3 \cdot 10^{-3}$ $cm^3 s^{-1}$ until the appearance of a bubble or cloud was observed. For each temperature the measurement was performed by triplicate. The standard uncertainty of the determination of the equilibrium pressure is estimated to be 0.10 MPa for bubble points and 0.15 MPa for cloud points.

Thus, visual observation for the mixture methane (1) + n-decane (2) with x_1=0.4031 was performed in the temperature range from (303.15 to 473.15) K, whereas for mixtures with x_1=0.6021 and x_1=0.8496 from (293.15 to 473.15) K. Also, constant mass expansion experiments (CME) were performed in the two-phase region by further expanding the system after the saturation pressure was reached. Consequently, several expansions were performed in the form of volume steps ranging

from 0.1 to 40 cm^3. In every step the mixture was stirred for 60 s and then subsequent waiting times of 600 s were applied until the pressure was stable within 0.05 MPa. Once stability was achieved, a photo of the mixture in the cell was taken by means of the Euclide software. Afterwards the liquid and gas volumes were measured from the photos taken in every step by means of the aforementioned software. This software measures the liquid level and uses this value to calculate the liquid volume by means of geometric formulas, the maximum standard uncertainty of the liquid fractions reported in this work is 0.009. A decrease in the liquid volume with expansion immediately after the saturation pressure indicated that the equilibrium point was a bubble point, whereas an increase of the liquid volume with expansion indicated a dew point.

2.2. Modeling

The experimental density and excess volume data presented in this work as well as the results on phase equilibrium of the binary mixtures methane + n-decane were modelled through the following EoSs: Soave-Redlich-Kwong [12], Peng-Robinson [13], Perturbed Chain Statistical Association Fluid Theory [14] and Soave-Benedict-Webb-Rubin EoS [15]. As concerns PC-SAFT, the simplified PC-SAFT EoS developed by von Solms et al. [24] was used in this work. The pure compound parameters of the aforementioned EoSs were taken from DIPPR database [25], except for PC-SAFT, for which the parameters were taken from the work of Gross and Sadowski [14]. These pure compound parameters are presented in Table 2. As concerns the methane/n-decane binary interaction parameters k_{ij} (Table 3), they were taken from Yan et al. [19] for the EoSs studied in this work.

Table 2
Pure compound parameters for SRK, PR, PC-SAFT and S-BWR EoSs.

	methane	n-decane
T_c / K*	190.56 [26]	617.70 [26]
p_c / MPa*	4.599 [26]	2.110 [26]
V_c / cm^3mol^{-1}*	98.6 [26]	617 [27]
ω*	0.0115 [28]	0.4923 [28]
σ / Å§	3.7039	3.8384
εk^{-1} / K§	150.03	243.87
m§	1	4.6627

*DIPPR database [25]
§Gross and Sadowski [14]

Table 3
Methane/n-decane binary interaction parameters, k_{ij}, for the EoSs studied in this work.

	SRK	PR	PC-SAFT	S-BWR
k_{ij}	0.0411*	0.0409*	0.0172*	-0.0311*

* Yan et al. [19]

3. Results and discussion

First of all it is worthy to note that in order to compare the experimental data obtained in this work with those from literature as well as with model calculations, bias, absolute average deviation (AAD), maximum deviation (D_{max}) and standard deviation (σ) were used, whose definition is given by the following equations:

$$\text{bias}/\% = \frac{100}{N}\sum_{i=1}^{N}\frac{Y_i^{ref/cal} - Y_i^{\exp}}{Y_i^{\exp}} \quad (4)$$

$$\text{AAD}/\% = \frac{100}{N}\sum_{i=1}^{N}\left|\frac{Y_i^{ref/cal} - Y_i^{\exp}}{Y_i^{\exp}}\right| \quad (5)$$

$$D_{max}/\% = 100\max\left(\frac{\left|Y_i^{ref/cal} - Y_i^{\exp}\right|}{Y_i^{\exp}}\right) \quad (6)$$

$$\sigma = \sqrt{\frac{\sum_{i=1}^{N}\left(Y_i^{\exp} - Y_i^{cal}\right)^2}{N-p}} \quad (7)$$

where $Y_i^{\exp}$ is the value of the experimental property determined in this work, $Y_i^{ref/cal}$ is the literature or the calculated value of the same property, N is the number of experimental data points and p is the number of parameters of the fit.

3.1. Density and excess volume

The quality of the density measurements was checked through the measurement of n-decane density from (278.15 to 398.15) K up to 140 MPa. Density values are included in table 4. These values were compared with the values previously reported in the literature by Lemmon and Span [29] and Cibulka and Hnědkovský [30], the obtained relative deviations are presented in Fig. 3.

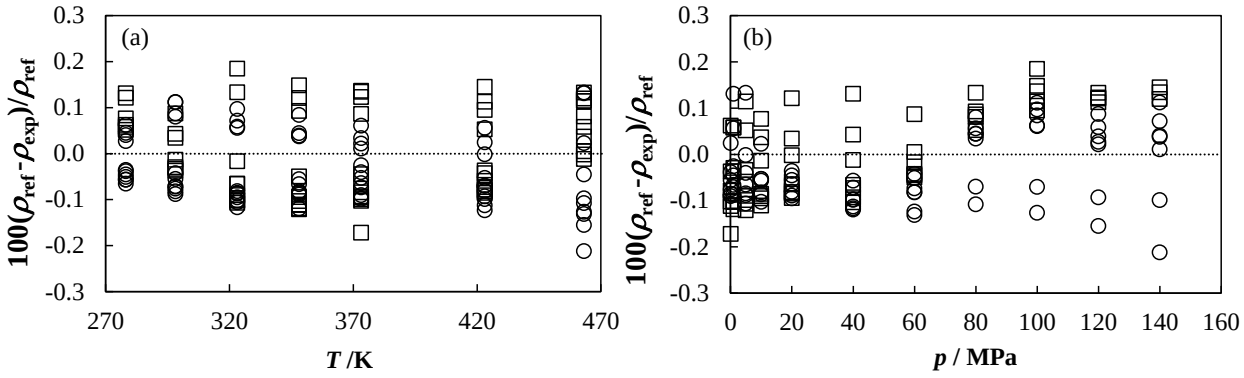

Fig. 3. Relative deviations between the density data measured in this work for n-decane and those from literature (a) against temperature and (b) against pressure. (□) Lemmon and Span [29] and (○) Cibulka and Hnědkovský [30].

The obtained density data for the binary system methane (1) + n-decane (2) are presented in Table 4. Moreover, the values of this property are depicted in Fig. 4 as a function of temperature at 80

MPa, and as a function of pressure at 323.15 K. The standard trends of density with temperature and pressure can be observed, that is, density decreases with temperature at constant pressure and increases with pressure at constant temperature. As regards the influence of methane mole fraction on this property, it is also as expected, density decreases with the increase of methane mole fraction in the binary mixture.

Table 4

Densities, ρ, of the binary mixture methane (1) + n-decane (2) in $g \cdot cm^{-3}$ at different temperatures and pressures[a]

	T/K						
p/MPa	278.15	298.15	323.15	348.15	373.15	423.15	463.15
	x_1= 0						
0.1	0.7416	0.7268	0.7078	0.6882	0.6686	0.6261	—
1.0	0.7423	0.7275	0.7086	0.6893	0.6693	0.6275	0.5910
5.0	0.7451	0.7306	0.7123	0.6935	0.6743	0.6347	0.6005
10.0	0.7483	0.7343	0.7165	0.6984	0.6800	0.6428	0.6113
20.0	0.7543	0.7409	0.7243	0.7073	0.6902	0.6562	0.6285
40.0	0.7656	0.7532	0.7381	0.7228	0.7074	0.6775	0.6538
60.0	0.7753	0.7636	0.7496	0.7354	0.7213	0.6941	0.6728
80.0	0.7834	0.7721	0.7588	0.7456	0.7325	0.7075	0.6880
100.0	0.7912	0.7804	0.7677	0.7551	0.7428	0.7193	0.7011
120.0	0.7989	0.7884	0.7763	0.7643	0.7525	0.7300	0.7127
140.0	0.8056	0.7954	0.7839	0.7725	0.7611	0.7394	0.7233
	x_1 = 0.2272						
10.0	0.7197	0.7045	0.6853	0.6654	0.6450	0.6027	0.5655
20.0	0.7266	0.7122	0.6945	0.6762	0.6576	0.6202	0.5891
40.0	0.7391	0.7260	0.7102	0.6940	0.6777	0.6458	0.6205
60.0	0.7499	0.7375	0.7230	0.7081	0.6933	0.6648	0.6426
80.0	0.7587	0.7469	0.7332	0.7194	0.7057	0.6798	0.6597
100.0	0.7671	0.7558	0.7428	0.7298	0.7169	0.6929	0.6742
120.0	0.7753	0.7644	0.7521	0.7396	0.7274	0.7044	0.6869
140.0	0.7825	0.7719	0.7602	0.7483	0.7366	0.7147	0.6985
	x_1 = 0.4520						
20.0	0.6798	0.6638	0.6437	0.6227	0.6008	0.5565	0.5204
40.0	0.6959	0.6817	0.6643	0.6466	0.6284	0.5931	0.5656
60.0	0.7084	0.6953	0.6796	0.6637	0.6476	0.6169	0.5935
80.0	0.7185	0.7061	0.6915	0.6769	0.6623	0.6347	0.6140
100.0	0.7279	0.7162	0.7024	0.6887	0.6751	0.6497	0.6307
120.0	0.7369	0.7257	0.7126	0.6997	0.6867	0.6627	0.6451
140.0	0.7447	0.7339	0.7215	0.7092	0.6969	0.6740	0.6579
	x_1 = 0.6017						
40.0	0.6531	0.6358	0.6161	0.5970	0.5777	0.5399	0.5103
60.0	0.6678	0.6520	0.6345	0.6177	0.6010	0.5688	0.5441
80.0	0.6796	0.6649	0.6488	0.6336	0.6186	0.5901	0.5683
100.0	0.6897	0.6760	0.6611	0.6470	0.6332	0.6070	0.5873
120.0	0.6991	0.6862	0.6724	0.6592	0.6462	0.6216	0.6033
140.0	0.7076	0.6954	0.6826	0.6703	0.6581	0.6348	0.6181
	x_1 = 0.7085						
40.0	0.5981	0.5822	0.5605	0.5382	0.5157	0.4730	0.4432

60.0	0.6163	0.6024	0.5839	0.5652	0.5467	0.5123	0.4883
80.0	0.6301	0.6174	0.6007	0.5842	0.5681	0.5385	0.5179
100.0	0.6421	0.6304	0.6150	0.5999	0.5853	0.5587	0.5403
120.0	0.6530	0.6421	0.6278	0.6137	0.6001	0.5754	0.5584
140.0	0.6624	0.6521	0.6387	0.6255	0.6127	0.5894	0.5737
	x_1 = 0.8496						
40.0	0.4949	0.4724	0.4508	0.4273	0.4050	0.3647	0.3345
60.0	0.5212	0.5048	0.4852	0.4651	0.4486	0.4124	0.3901
80.0	0.5394	0.5244	0.5075	0.4902	0.4762	0.4446	0.4252
100.0	0.5540	0.5403	0.5252	0.5095	0.4971	0.4688	0.4511
120.0	0.5669	0.5539	0.5404	0.5258	0.5140	0.4883	0.4708
140.0	0.5779	0.5653	0.5529	0.5394	0.5273	0.5037	0.4871

[a]Expanded density uncertainty $U(\rho)$ (k=2): $0.7\cdot10^{-3}$ g·cm^{-3} at T < 373.15 K; $5\cdot10^{-3}$ g·cm^{-3} at $T \geqslant$ 373.15 K and p = 0.1 MPa; $5\cdot10^{-3}$ g·cm^{-3} at T = 463.15 K and p = 1MPa; $3\cdot10^{-3}$ g·cm^{-3} at other temperature and pressure conditions. Expanded mole fraction uncertainty $U(x)$ (k=2): $3\cdot10^{-4}$; standard temperature uncertainty $u(T)$: 0.02 K; standard pressure uncertainty $u(p)$: 0.08 MPa.

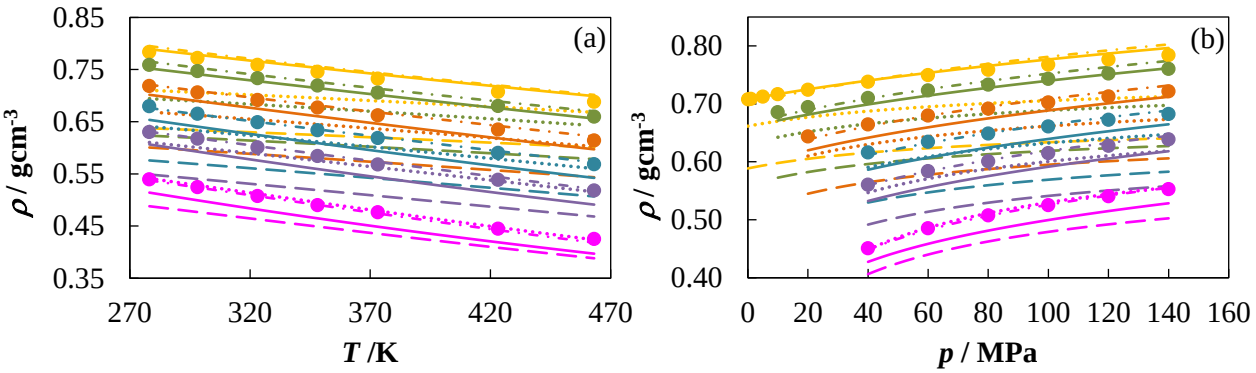

Fig. 4. Density of the binary mixtures methane (1) + n-decane (2) (a) as a function of temperature at 80 MPa and (b) as a function of pressure at 323.15 K. (●) x_1=0, (●) x_1=0.2272, (●) x_1=0.4520, (●) x_1=0.6017, (●) x_1=0.7085 and (●) x_1=0.8496. (---) SRK EoS, (···) PR EoS, (-·-) PC-SAFT EoS and (–) S-BWR EoS.

The experimental density values obtained in this work have been correlated as a function of temperature and pressure by means of the following modified Tammann-Tait equation:

$$\rho(T,p) = \frac{\rho(T,p_{ref})}{1 - C\cdot\ln\left(\dfrac{B(T)+p}{B(T)+p_{ref}}\right)} \tag{8}$$

where $\rho(T, p_{ref})$ is the density as a function of temperature at a reference pressure, given by the following polynomial equation:

$$\rho(T,p_{ref}) = \sum_{i=0}^{N} A_i T^i \tag{9}$$

C is a parameter independent of temperature and pressure and $B(T)$ is a temperature dependent parameter given by the following polynomial equation:

$$B(T) = \sum_{j=0}^{n} B_j T^j \tag{10}$$

The parameters obtained for the fit are presented in table 5, along with the absolute average deviation and the standard deviations of the fit, σ for $\rho(T, p_{ref})$ and σ^* for $\rho(T, p)$.

Table 5

Fitting parameters of the modified Tammann-Tait equation (Eq. 8), standard deviations σ (Eq. 9) and σ^* (Eq. 8), and AAD for the density of the binary mixtures methane (1) + n-decane (2).

	$x_1 = 0$	$x_1 = 0.2272$	$x_1 = 0.4520$	$x_1 = 0.6017$	$x_1 = 0.7085$	$x_1 = 0.8496$
p_{ref} / MPa	0.1	10	20	40	40	40
A_0 /g·cm^{-3}	0.9055	0.8823	0.8066	0.9724	0.5536	0.8384
$10^4 \cdot A_1$ /g·cm^{-3}·K^{-1}	-4.54	-4.38	-0.33	-15.78	16.18	-14.65
$10^7 \cdot A_2$ /g·cm^{-3}·K^{-2}	-4.86	-5.3	-19.1	19.764	-70.95	8.2
$10^9 \cdot A_3$ /g·cm^{-3}·K^{-3}	0.00	0.00	1.395	-1.56	6.664	0.00
$10^3 \cdot \sigma$/ g·cm^{-3}	0.2	0.4	0.2	0.4	0.2	1.0
C	0.0875	0.0884	0.091	0.1076	0.109	0.1205
B_0 /MPa	355.6	324.3	280.29	304.1	258.4	139.3
B_1 /MPa·K^{-1}	-1.262	-1.189	-1.1063	-1.231	-1.151	-0.703
$10^3 \cdot B_2$ /MPa·K^{-2}	1.16	1.09	1.053	1.172	1.161	0.721
$10^3 \cdot \sigma^*$ / g·cm^{-3}	0.5	0.4	0.7	0.4	0.7	2.4
AAD / %	0.05	0.04	0.08	0.09	0.08	0.36

Density data of the studied binary system have been previously reported in literature. Auddonet and Pádua [4] have measured density in the temperature range from (303.15 to 393.15)K up to 76 MPa for binary mixtures with methane mole fractions of 0.227, 0.410, 0.601 and 0.799. Moreover Canet et al. [11] have measured density values for this binary system in the temperature range from (293.15 to 373.15)K at pressures up to 60 MPa for methane mole fractions of 0.3124, 0.4867, 0.6000, 0.7566 and 0.9575. These last authors [11] have also reported extrapolated density values through a Tait type equation up to 140 MPa.

The correlated density values obtained in this work have been compared with the aforementioned literature data on this binary system for methane mole fractions of 0.2 and 0.6, which are the ones closed to those reported in this work. The relative deviations obtained are plotted in Fig. 5. For x_1=0.2, the comparison with the density data previously reported by Audonnet and Pádua [4] yielded a bias of -0.01%, a maximum deviation of 0.42% and an absolute average deviation of 0.13%. As concerns x_1=0.6, the comparison with data from Audonnet and Pádua [4] as well as from Canet et al. [11] yielded a bias of 0.09%, a maximum deviation of 0.81% and an absolute average deviation of 0.18%. This comparison shows that the deviations with previously reported density data are within the combined uncertainty of the experimental techniques.

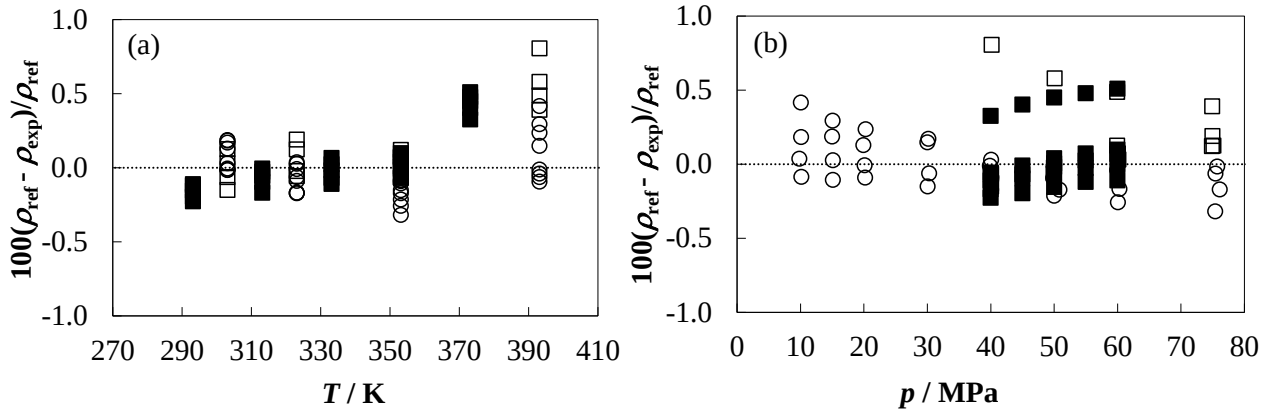

Fig. 5. Relative deviations between the density data measured in this work for the binary system methane (1) + n-decane (2) and those from literature (a) against temperature and (b) against pressure. (○) x_1=0.2 and (□, ■) x_1=0.6. Filled symbols represent the relative deviation with data from Canet et al. [11] and empty symbols with data from Audonnet and Pádua [4].

Four different equations of state have been used to calculate the density values reported in this work, i.e. SRK, PR, PC-SAFT and S-BWR. The calculated density values through the different EoSs at 80 MPa in the whole temperature range, as well as at 323.15 K in the whole pressure range are depicted in Fig. 4 (a) and Fig. 4 (b), respectively. A quantitative summary of the density calculation results is gathered in table 6, where bias and maximum deviation, as well as the absolute average deviation are presented. It can be observed that the best results for this property are obtained through the PC-SAFT EoS, which yielded an AAD of 0.9 % with a maximum deviation of 4 %. On the other hand, the poorest density results were obtained through the SRK EoS, which yielded an AAD of 14% with a maximum deviation of 20%. Additionally in Fig. 6, the performance of the different models is presented as a function of the methane mole fraction (x_1) in the binary mixture. For both SRK and PR the density results turn better as methane mole fraction increases in the binary mixture, on the contrary for S-BWR, the results become poorer as methane mole fraction increases in the binary mixture. As concerns PC-SAFT, no trend is observed on the quality of the density results with methane mole fraction.

Table 6

Bias, absolute average deviation and maximum deviations for the calculated densities of the binary system methane + n-decane in the whole experimental (p,T,x) range through the different EoSs.

	bias / %	AAD / %	D_{max} / %
SRK	-14	14	20
PR	-4.2	4.3	11
PC-SAFT	0.5	0.9	4.0
S-BWR	-2.2	2.6	7.1

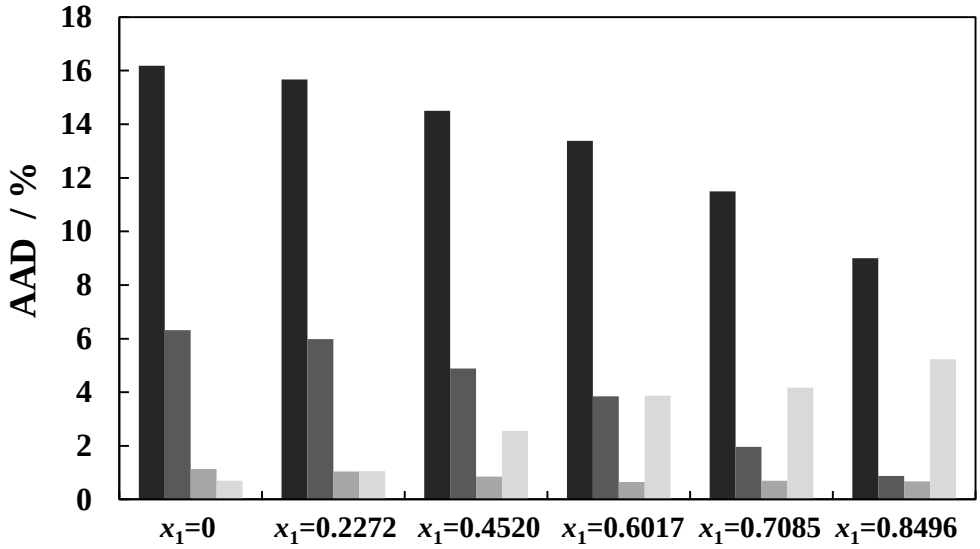

Fig. 6. Absolute average deviations (AAD) for the calculated densities of the binary system methane (1) + n-decane (2) in the whole experimental (*T*,*p*) range. (■) SRK, (■) PR, (■) PC-SAFT and (■) S-BWR.

Excess volumes (V^E) were calculated from the experimental density data according to the following equation:

$$V^E = \frac{x_1 M_1 + (1-x_1) M_2}{\rho} - \left(\frac{x_1 M_1}{\rho_1} + \frac{(1-x_1) M_2}{\rho_2} \right) \tag{11}$$

where x_1 is the mole fraction of methane, M_1 and M_2 are the molecular weights of methane and n-decane, respectively. ρ, ρ_1 and ρ_2 are density values of the mixture, methane and n-decane, respectively.

It should be noted that as we did not measure the density values of methane in the present work, these values were taken from Setzmann and Wagner [31] in order to obtain the excess volumes. The obtained excess volumes are reported in table 7. They are negative in the whole (*p*,*T*,*x*) range, and become more negative as the pressure decreases or the temperature increases for a given composition of the binary mixture. The same trend of the excess volume with temperature and pressure has been reported by us in a previous work [10] for the binary systems n-hexane + n-decane and n-hexane + n-hexadecane. Moreover, Katzenski and Schneider [32] studied excess volumes of n-alkane binaries from 10 to 200 MPa at 298.15 K and found also negative excess volumes which became less negative with increasing pressure and approached zero at the highest pressures of their study. Also Schneider [33] presented the fact that the absolute value of excess volume becomes closer to zero when increasing pressure for binary alkane mixtures. Similarly, Lepori et al. [34] analysed the excess molar volume of 40 binary mixtures containing heptane plus a liquid alkane at 298.15 K, finding mainly negative excess volumes attributed to the different free volume of the mixture components. They also stated that as the mixture become more asymmetric the tight packing of different molecule sizes becomes more and more important which is reflected in a more negative excess volume. As concerns the trend with temperature, it was already reported

by Apam-Martínez and Trejo [35] after the study of the excess volume of several alkane binaries, that for a given mixture the magnitude of the excess volume increases with temperature.

Considering the excess volume values obtained in this work for pressures equal or higher than 40 MPa (in order to have data on excess volume for all the studied compositions), the minimum of this property is found to be -21.7 cm^3mol^{-1}, for the mixture with x_1=0.6017 at 463.15 K and 40 MPa. Also, the excess volume of the studied binary mixtures in the whole temperature range for pressures higher or equal to 40 MPa represents up to a 19% of the molar volume at a given temperature and pressure condition. This maximum percentage is found for the binary mixture with x_1=0.8496 at the temperatures of 423.15 K and 463.15 K and pressure of 40 MPa. Values of the excess volume are depicted in Fig. 7 at 278.15 K and 463.15 K. It can be observed that this property is asymmetric with respect to the methane mole fraction, and the minimum is displaced towards higher mole fraction of the lighter compound in the binary mixture. We have already observed this kind of behavior in a previous study of another asymmetric alkane binary mixture, i.e. n-hexane + n-hexadecane [10]. This last mixture was also studied by Trejo-Rodríguez and Paterson [36] who concluded that the skewing of the excess volume curves towards the lighter alkane mole fraction is related to the difference in the chain length of both alkanes, the large free volume of the light alkane and the high orientational order of the heavier alkane.

Table 7

Excess volume, V^E (cm^3mol^{-1}), for the binary system methane (1) + n-decane (2)[a]

	T/K						
p/MPa	278.15	298.15	323.15	348.15	373.15	423.15	463.15
	x_1= 0.2272						
10.0	-31.1	-36.5	-42.4	-47.8	-52.6	-61.1	-66.2
20.0	-9.68	-12.1	-15.1	-17.7	-20.1	-24.2	-26.7
40.0	-3.55	-4.19	-5.12	-6.02	-6.90	-8.55	-9.64
60.0	-2.14	-2.42	-2.88	-3.29	-3.71	-4.55	-5.15
80.0	-1.50	-1.65	-1.93	-2.17	-2.40	-2.92	-3.31
100.0	-1.15	-1.24	-1.43	-1.58	-1.73	-2.09	-2.37
120.0	-0.93	-0.99	-1.14	-1.23	-1.33	-1.61	-1.85
140.0	-0.78	-0.82	-0.94	-1.00	-1.07	-1.31	-1.54
	x_1 = 0.4520						
20.0	-18.3	-23.0	-28.6	-33.6	-37.9	-44.9	-49.0
40.0	-6.47	-7.72	-9.41	-11.1	-12.6	-15.5	-17.4
60.0	-3.77	-4.33	-5.11	-5.88	-6.59	-8.02	-9.15
80.0	-2.56	-2.88	-3.32	-3.75	-4.14	-5.00	-5.76
100.0	-1.90	-2.10	-2.39	-2.66	-2.90	-3.47	-4.04
120.0	-1.50	-1.64	-1.84	-2.02	-2.17	-2.58	-3.06
140.0	-1.21	-1.31	-1.46	-1.59	-1.69	-2.02	-2.46
	x_1 = 0.6017						
40.0	-8.53	-9.82	-11.8	-13.9	-15.9	-19.5	-21.7
60.0	-5.08	-5.51	-6.35	-7.32	-8.27	-10.1	-11.4
80.0	-3.57	-3.72	-4.16	-4.72	-5.28	-6.38	-7.24
100.0	-2.67	-2.71	-2.98	-3.35	-3.72	-4.47	-5.10

120.0	-2.09	-2.09	-2.30	-2.58	-2.85	-3.39	-3.89
140.0	-1.72	-1.72	-1.90	-2.14	-2.36	-2.79	-3.25
	x_1 = 0.7085						
40.0	-8.28	-10.1	-12.2	-14.1	-15.8	-18.6	-20.7
60.0	-4.60	-5.46	-6.36	-7.21	-8.01	-9.63	-11.2
80.0	-3.01	-3.53	-4.02	-4.49	-4.96	-6.04	-7.22
100.0	-2.16	-2.53	-2.83	-3.12	-3.44	-4.24	-5.18
120.0	-1.64	-1.94	-2.16	-2.36	-2.58	-3.19	-3.96
140.0	-1.28	-1.54	-1.71	-1.86	-2.02	-2.50	-3.16
	x_1 = 0.8496						
40.0	-8.07	-9.17	-11.5	-13.4	-15.2	-18.4	-19.8
60.0	-4.58	-5.24	-6.14	-6.91	-8.14	-9.46	-11.3
80.0	-3.06	-3.36	-3.92	-4.37	-5.23	-6.07	-7.43
100.0	-2.22	-2.41	-2.82	-3.09	-3.76	-4.37	-5.41
120.0	-1.75	-1.83	-2.20	-2.38	-2.87	-3.39	-4.05
140.0	-1.40	-1.43	-1.75	-1.90	-2.17	-2.64	-3.15

[a]Expanded uncertainty of the excess volume $U(V^E)$ (k=2): 0.06 – 3.18 cm^{3}mol^{-1}

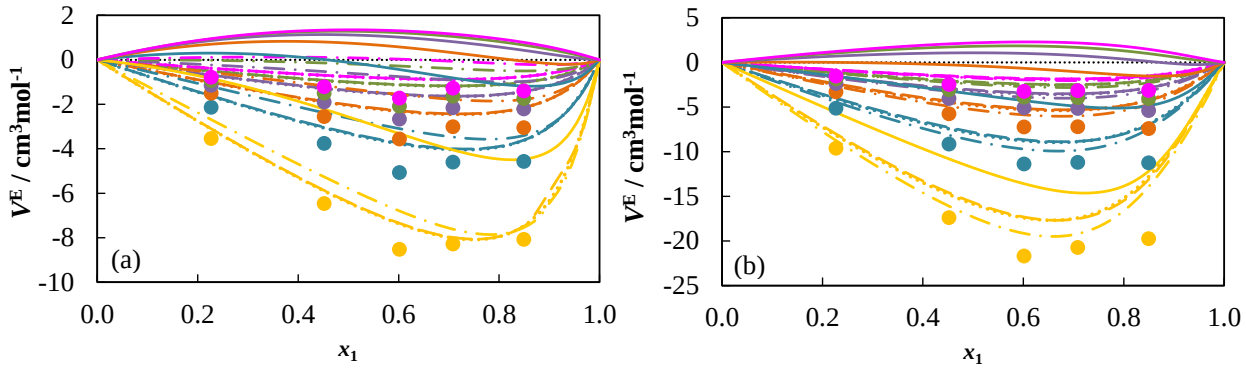

Fig. 7. Excess volume for the binary system methane (1) + n-decane (2) at (a) 278.15 K and (b) 463.15 K. (●) 40 MPa, (●) 60 MPa, (●) 80 MPa, (●) 100 MPa, (●) 120 MPa and (●) 140 MPa. (---) SRK EoS, (···) PR EoS, (-·-) PC-SAFT EoS, (−) S-BWR EoS.

The values of the excess volume for the system studied in this work have been calculated by SRK, PR, PC-SAFT and S-BWR. Results are plotted in Fig. 7 along with the experimental data for this property at two temperatures (278.15 K and 463.15 K) at different pressures. The best calculation results for the experimental V^E values were obtained by SRK and PR (AADs of 26% and 25%, respectively), whereas PC-SAFT yields an AAD of 33% and calculations through S-BWR are the poorest (AAD of 106%).

3.2. Density derived properties

Isothermal compressibility (κ_T) has been calculated by differentiation of the Tammann-Tait correlation of density as a function of temperature and pressure (Eq. 8), according to the following equation:

$$\kappa_T(T,p)=\frac{1}{\rho}\left(\frac{\partial\rho}{\partial p}\right)_T \tag{12}$$

The obtained κ_T values are presented in table 8. Moreover, in Fig. 8 it is plotted the dependence of this property on pressure at two different temperatures, 323.15 K and 463.15 K, thus it is possible to see how the different variables affect isothermal compressibility values. As expected, this property increases with the increase in the methane mole fraction in the mixture or in the temperature, whereas it decreases when the pressure increases. We have compared the compressibility values of n-decane (x_1=0) reported in this work with those we have published in a previous work [10] in the whole temperature range and pressures up to 50 MPa finding an AAD of 1.9% which is within the combined uncertainty of the reported values. Additionally we have compared the isothermal compressibility values of the binary mixtures studied in this work (from x_1=0 to x_1=0.8496) with those reported by the NIST Standard Reference Database 23, Version 9.1. The values reported for n-decane in the aforementioned database are obtained by using the EoS reported by Lemmon and Span [29] whereas for the binary mixtures methane (1) + n-decane (2) the κ_T values reported in the database are obtained according to GERG-2008 EoS [37]. The AAD obtained in the comparison is 5.3%. The values reported by the NIST database are plotted as well in Fig. 8 at 323.15 K and 463.15 K and it is possible to see the agreement with the values obtained in this work.

Table 8

Isothermal compressibility values, $10^3\kappa_T$ (MPa^{-1}), for the binary system methane (1) + n-decane (2)[a]

	T/K						
p/MPa	278.15	298.15	323.15	348.15	373.15	423.15	463.15
	x_1= 0						
1.0	0.92	1.05	1.25	1.51	1.86	2.90	–
5.0	0.88	1.01	1.19	1.43	1.72	2.59	3.58
10.0	0.85	0.96	1.12	1.33	1.58	2.29	3.03
20.0	0.78	0.87	1.01	1.17	1.36	1.86	2.33
40.0	0.67	0.74	0.84	0.95	1.07	1.37	1.61
60.0	0.59	0.65	0.72	0.80	0.89	1.09	1.25
80.0	0.53	0.57	0.63	0.69	0.76	0.90	1.02
100.0	0.48	0.52	0.56	0.61	0.67	0.78	0.87
120.0	0.44	0.47	0.51	0.55	0.59	0.68	0.75
	x_1= 0.2272						
20.0	0.91	1.03	1.21	1.44	1.72	2.50	3.36
40.0	0.77	0.85	0.97	1.12	1.28	1.68	2.04
60.0	0.67	0.73	0.82	0.92	1.03	1.28	1.49
80.0	0.59	0.64	0.71	0.78	0.86	1.04	1.18
100.0	0.53	0.57	0.62	0.68	0.74	0.87	0.98
120.0	0.48	0.51	0.56	0.60	0.65	0.76	0.84
	x_1= 0.4520						
40.0	0.99	1.11	1.29	1.50	1.76	2.38	2.93
60.0	0.83	0.91	1.03	1.17	1.32	1.66	1.93
80.0	0.72	0.78	0.87	0.96	1.07	1.29	1.46

100.0	0.63	0.68	0.75	0.82	0.90	1.06	1.18
120.0	0.57	0.61	0.66	0.72	0.78	0.90	0.99
	x_1= 0.6017						
60.0	0.98	1.09	1.25	1.43	1.65	2.14	2.53
80.0	0.85	0.93	1.04	1.17	1.31	1.61	1.83
100.0	0.75	0.81	0.90	0.99	1.09	1.30	1.45
120.0	0.67	0.72	0.79	0.86	0.94	1.10	1.21
	x_1= 0.7085						
60.0	1.27	1.44	1.67	1.96	2.28	3.01	3.51
80.0	1.06	1.17	1.33	1.51	1.70	2.10	2.35
100.0	0.91	1.00	1.11	1.23	1.37	1.63	1.79
120.0	0.80	0.87	0.96	1.05	1.15	1.34	1.45
	x_1= 0.8496						
60.0	2.13	2.37	2.72	3.12	3.55	4.46	4.98
80.0	1.65	1.80	2.00	2.22	2.45	2.91	3.16
100.0	1.36	1.46	1.60	1.75	1.90	2.19	2.36
120.0	1.16	1.24	1.34	1.45	1.56	1.78	1.90

[a]Relative expanded isothermal compressibility uncertainty $U_r(\kappa_T)$ (k=2): 0.02

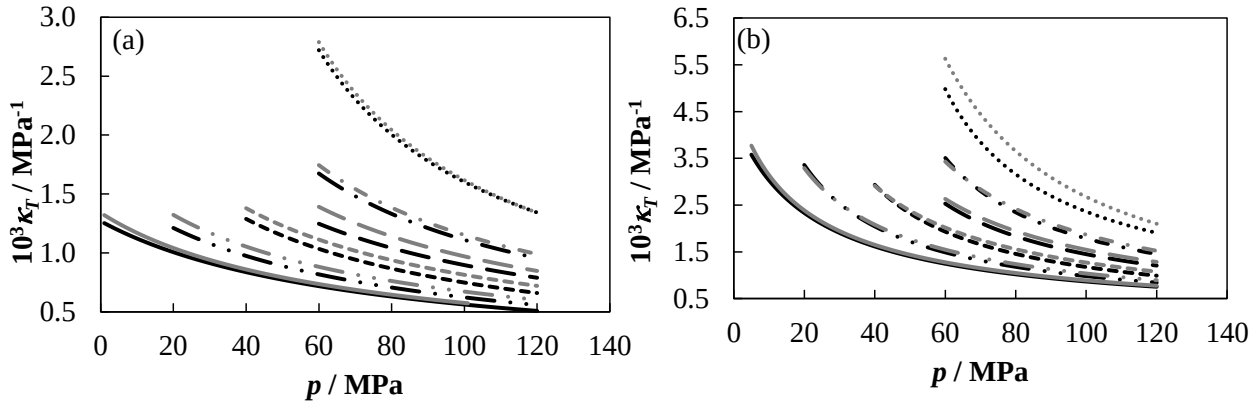

Fig. 8. Isothermal compressibility (κ_T) of the binary mixture methane (1) + n-decane (2) at (a) 323.15 K and at (b) 463.15 K. (—) x_1=0, (—··—) x_1=0.2272, (---) x_1=0.4520, (— —) x_1=0.6017, (-·-) x_1=0.7085 and (···) x_1=0.8496. Black lines represent the values obtained in this work by differentiation, whereas the grey lines represent the values reported by the NIST Standard Reference Database 23, Version 9.1.

We have also calculated the isobaric thermal expansion coefficient (α_p) from the experimental density data. This property is defined as follows:

$$\alpha_p(T,p) = -\frac{1}{\rho}\left(\frac{\partial\rho}{\partial T}\right)_p \qquad (13)$$

It has been recommended [20] to derive this coefficient from the correlation of the isobaric densities as a function of temperature rather than from the Tammann-Tait equation (Eq. 8), because in this last case the obtained isobaric thermal expansivity values depend on the form of the functions used for $\rho(T, p_{ref})$ and $B(T)$. Thus, in this work, we have correlated the densities as a function of

temperature along each isobar by means of a second degree polynomial according to the following equation:

$$\rho_p(T) = D_0 + D_1 T + D_2 T^2 \quad (14)$$

The isobaric densities for every binary mixture have been fitted through Eq. 14 with standard deviations lower or equal to $1 \cdot 10^{-3}$ g·cm^{-3} (Table S1 in the supplementary information). Afterwards the obtained fitting parameters were used to obtain the isobaric thermal expansion coefficients as follows:

$$\alpha_p(T) = -\frac{D_1 + 2D_2 T}{D_0 + D_1 T + D_2 T^2} \quad (15)$$

The α_p values obtained for the binary mixtures are presented in table 9. Under the same temperature and pressure conditions this coefficient increases with the increase of the methane mole fraction in the binary mixture, as this property decreases with the increase of the alkyl chain length of alkanes [38]. It can also be observed in table 9 that this property increases with temperature along isobars at pressures up to 40 or 60 MPa, whereas it decreases with temperature at higher pressures. As concerns the pressure dependence along isotherms, it was found that this property decreases with pressure at constant temperature. These trends of α_p with temperature and pressure are expected when the experimental conditions are not in the vicinity of the critical point [38]. It is interesting to note that the combination of these temperature and pressure dependences of the isobaric thermal expansion coefficient leads to a crossover region among the isotherms of the α_p vs. p plot [38]. Thus, in Fig. 9 the isobaric thermal expansion coefficient is depicted against pressure at different temperatures for all the studied binary mixtures. It can be seen the mentioned crossover region between the isotherms for all of the analysed systems.

Table 9

Isobaric thermal expansion coefficient, $10^3\alpha_p$ (K^{-1}), for the binary system methane (1) + n-decane (2)[a]

	T/K				
p/MPa	298.15	323.15	348.15	373.15	423.15
	$x_1 = 0$				
0.1	1.02	1.09	1.15	1.22	1.38
1.0	1.01	1.08	1.15	1.22	1.39
5.0	0.99	1.04	1.10	1.16	1.30
10.0	0.96	1.00	1.04	1.09	1.19
20.0	0.90	0.93	0.96	0.99	1.05
40.0	0.82	0.83	0.84	0.85	0.88
60.0	0.75	0.76	0.76	0.77	0.78
80.0	0.71	0.71	0.70	0.70	0.70
100.0	0.67	0.66	0.66	0.65	0.64
120.0	0.63	0.63	0.62	0.62	0.60
140.0	0.60	0.60	0.59	0.58	0.56
	$x_1 = 0.2272$				
10.0	1.07	1.14	1.21	1.29	1.47
20.0	1.00	1.04	1.08	1.13	1.23
40.0	0.89	0.91	0.93	0.95	0.99
60.0	0.82	0.82	0.83	0.84	0.85
80.0	0.76	0.76	0.76	0.76	0.75
100.0	0.71	0.71	0.70	0.70	0.68

120.0	0.68	0.67	0.66	0.65	0.64
140.0	0.64	0.63	0.62	0.61	0.59
	x_1 = 0.4520				
20.0	1.22	1.29	1.36	1.44	1.62
40.0	1.04	1.07	1.09	1.12	1.18
60.0	0.93	0.94	0.95	0.96	0.98
80.0	0.86	0.86	0.85	0.85	0.85
100.0	0.80	0.79	0.79	0.78	0.76
120.0	0.75	0.74	0.73	0.72	0.70
140.0	0.71	0.70	0.69	0.67	0.64
	x_1 = 0.6017				
40.0	1.26	1.28	1.31	1.33	1.38
60.0	1.11	1.11	1.10	1.10	1.10
80.0	1.00	0.99	0.97	0.96	0.93
100.0	0.91	0.90	0.88	0.86	0.82
120.0	0.84	0.83	0.81	0.79	0.75
140.0	0.78	0.76	0.75	0.73	0.69
	x_1 = 0.7085				
40.0	1.53	1.56	1.60	1.64	1.73
60.0	1.26	1.27	1.27	1.28	1.28
80.0	1.11	1.10	1.09	1.07	1.04
100.0	1.00	0.98	0.96	0.94	0.90
120.0	0.91	0.90	0.88	0.86	0.81
140.0	0.85	0.83	0.81	0.79	0.74
	x_1 = 0.8496				
40.0	2.07	2.08	2.10	2.12	2.13
60.0	1.62	1.61	1.60	1.58	1.54
80.0	1.36	1.34	1.32	1.29	1.24
100.0	1.19	1.17	1.14	1.11	1.06
120.0	1.06	1.04	1.03	1.00	0.96
140.0	0.98	0.96	0.94	0.92	0.87

[a]Relative expanded isobaric thermal expansion coefficient uncertainty $U_r(\alpha_p)$ (k=2): 0.03

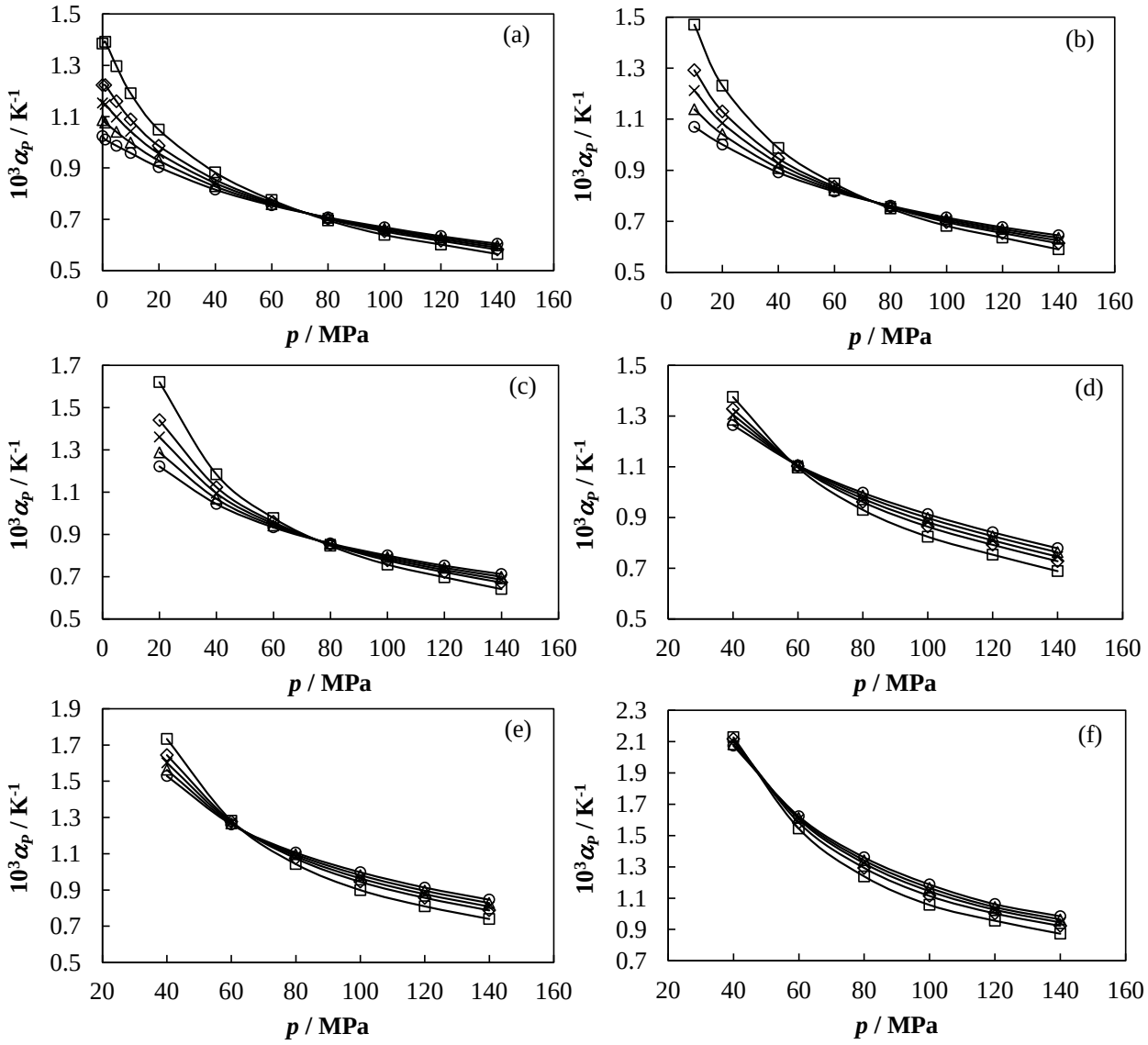

Fig. 9. Isobaric thermal expansion coefficient (α_p) for the binary systems methane (1) + n-decane (2) at (○) 298.15 K, (△) 323.15 K, (×) 348.15 K, (◇) 373.15 K and (□) 423.15 K. (a) x_1=0, (b) x_1=0.2272, (c) x_1=0.4520, (d) x_1=0.6017, (e) x_1=0.7085 and (f) x_1=0.8496. Solid lines are depicted to guide the eye.

3.3. Phase equilibrium

As concerns the phase equilibrium, the saturation pressures obtained through visual observation are presented in table 10. In the whole range of studied temperatures for mixtures with x_1=0.4031 and x_1=0.6021, the observed phase change when decreasing pressure at constant temperature was always a bubble point. For the mixture with x_1=0.8496, a cloud point was observed at the saturation pressure in the whole studied temperature range. More specifically for this last mixture, in the temperature range from (293.15 to 377.14) K the appearance of a vapor phase was observed after the cloud subsided. For the temperature range from (443.70 to 472.12) K the appearance of a liquid

phase was observed when decreasing pressure at constant temperature. Finally, for temperatures between 397.96 K and 422.85 K it was not easy to evaluate whether the phase change observed was a bubble or a dew point, since when the cloud vanished the volume of the new phase was quite large. For this reason, the measurements of the liquid fraction (V_{liquid}/V_{total}) as a function of pressure in the two-phase region following the procedure described in the experimental section were used to determine the type of phase transition observed. The liquid fraction data measured for the three binary mixtures are presented in tables 11 to 13. According to the data on table 13, it is possible to confirm that at 397.96 K the phase change when decreasing pressure at constant temperature is from liquid to liquid + vapor (bubble point), whereas at 410.66 K and 422.85 K the phase change is from vapor to vapor + liquid (dew point).

Table 10

Saturation pressures of the binary system methane (1) + n-decane (2)[a]

T / K	p / MPa	T / K	p / MPa	T / K	p / MPa
		x_1=0.4031			
303.18	11.30	347.96	12.92	422.89	13.78
310.94	11.66	377.27	13.49	443.75	13.70
323.08	12.13	398.00	13.70	472.14	13.42
338.01	12.66	410.66	13.77		
		x_1=0.6021			
294.12	21.15	348.09	23.29	423.09	23.11
303.19	21.65	373.10	23.59	444.40	22.45
311.04	22.03	377.30	23.61	448.11	22.31
323.17	22.55	394.17	23.57	472.47	21.14
344.22	23.22	410.85	23.36		
		x_1=0.8496			
293.15	35.94	333.42	35.52	422.85	30.06*
298.21	35.98	349.99	35.04	443.70	27.81*
303.19	35.96	377.14	33.66	472.12	24.41*
310.92	35.90	397.96	32.21		
320.70	35.78	410.66	31.16*		

*Dew points

[a]Standard temperature uncertainty $u(T)$: 0.02 K; Standard pressure uncertainty $u(p)$: 0.10 MPa for the mixtures with x_1=0.4031 and x_1=0.6021 and 0.15 MPa for the mixture with x_1=0.8496.

Table 11

Liquid fraction (V_{liquid}/V_{total}) for the system methane (1) + n-decane (2) with x_1 = 0.4031[a]

p/MPa	Liquid fraction	p/MPa	Liquid fraction	p/MPa	Liquid fraction
T = 303.17 K		T = 310.92 K		T = 323.05 K	
11.25	0.997	11.59	0.998	12.11	0.998
11.03	0.991	11.36	0.991	11.88	0.992
10.60	0.975	10.92	0.974	11.45	0.976
9.86	0.937	10.18	0.938	10.67	0.940
8.47	0.860	8.75	0.863	9.19	0.868
6.70	0.737	6.92	0.740	7.28	0.743
4.83	0.584	4.95	0.588	5.21	0.587

3.79	0.489	3.88	0.493	4.08	0.493
T = 337.97 K		T = 347.91 K		T = 377.14 K	
12.55	0.997	12.91	0.998	13.47	0.998
12.32	0.990	12.68	0.992	13.25	0.991
11.88	0.973	12.23	0.976	12.83	0.976
11.10	0.937	11.44	0.941	12.06	0.944
9.59	0.866	9.90	0.868	10.53	0.868
7.61	0.745	7.87	0.744	8.45	0.748
5.45	0.589	5.63	0.592	6.11	0.595
4.27	0.492	4.41	0.496	4.80	0.498
T = 397.97 K		T = 410.66 K		T = 422.87 K	
13.58	0.995	13.65	0.994	13.69	0.995
13.17	0.978	13.24	0.978	13.30	0.979
12.43	0.946	12.53	0.946	12.61	0.947
10.92	0.876	11.05	0.869	11.18	0.872
8.82	0.755	8.98	0.753	9.14	0.753
6.43	0.600	6.57	0.600	6.72	0.605
5.07	0.501	5.20	0.502	5.34	0.506
T = 443.72 K		T = 472.15 K			
13.67	0.997	13.24	0.993		
13.32	0.982	12.94	0.976		
12.68	0.949	12.39	0.945		
11.32	0.873	11.21	0.869		
9.36	0.757	9.43	0.752		
6.98	0.608	7.18	0.605		
5.59	0.506	5.83	0.507		

[a]Standard temperature uncertainty $u(T)$: 0.02 K; Standard pressure uncertainty $u(p)$: 0.06 MPa; Standard liquid fraction uncertainty u(Liquid fraction): 0.009.

Table 12

Liquid fraction (V_{liquid}/V_{total}) for the system methane (1) + n-decane (2) with x_1 = 0.602 [a]

p/MPa	Liquid fraction	p/MPa	Liquid fraction	p/MPa	Liquid fraction
T = 303.19 K		T = 311.11 K		T = 323.23 K	
21.18	0.995	21.52	0.993	22.17	0.995
20.55	0.979	20.93	0.977	21.59	0.980
19.42	0.947	19.84	0.945	20.55	0.950
17.60	0.890	18.07	0.891	18.79	0.894
14.53	0.783	14.99	0.778	15.70	0.783
11.11	0.640	11.49	0.643	12.08	0.645
7.79	0.486	8.06	0.484	8.47	0.488
6.08	0.397	6.28	0.399	6.57	0.396
T = 344.31 K		T = 348.18 K		T = 372.95 K	
22.96	0.997	23.00	0.996	23.36	0.996
22.43	0.982	22.48	0.979	22.91	0.981
21.46	0.952	21.56	0.948	22.06	0.949
19.80	0.896	19.91	0.891	20.56	0.896
16.72	0.785	16.87	0.785	17.67	0.786

12.96	0.644	13.12	0.645	13.92	0.647
9.12	0.491	9.24	0.490	9.90	0.492
7.08	0.404	7.19	0.399	7.74	0.401
T = 377.32 K		T = 394.18 K		T = 410.88 K	
22.91	0.980	22.97	0.980	22.83	0.985
22.11	0.949	22.20	0.949	22.12	0.953
20.62	0.893	20.83	0.895	20.84	0.898
17.76	0.783	18.10	0.784	18.25	0.782
14.04	0.645	14.44	0.650	14.69	0.647
10.01	0.490	10.39	0.494	10.66	0.491
7.82	0.399	8.15	0.401	8.40	0.401
T = 423.09 K		T = 444.37 K		T = 448.13 K	
22.78	0.988	22.15	0.994	21.98	0.983
22.13	0.956	21.57	0.968	21.43	0.949
20.91	0.899	20.51	0.924	20.40	0.890
18.42	0.784	18.28	0.845	18.22	0.776
14.94	0.645	15.05	0.739	15.05	0.636
10.91	0.494	11.17	0.623	11.21	0.486
8.63	0.403	8.91	0.482	8.97	0.399
T = 472.53 K					
21.04	0.996				
20.58	0.955				
19.71	0.891				
17.82	0.770				
14.98	0.631				
11.40	0.477				
9.23	0.388				

[a]Standard temperature uncertainty $u(T)$: 0.02 K; Standard pressure uncertainty $u(p)$: 0.06 MPa; Standard liquid fraction uncertainty u(Liquid fraction): 0.009.

Table 13

Liquid fraction (V_{liquid}/V_{total}) for the system methane (1) + n-decane (2) with x_1 = 0.8496[a]

p/MPa	Liquid fraction	p/MPa	Liquid fraction	p/MPa	Liquid fraction
T = 293.15 K		T = 298.21 K		T = 303.19 K	
35.74	0.925	35.74	0.929	35.75	0.932
35.01	0.809	35.03	0.807	35.12	0.814
33.54	0.710	33.62	0.709	33.77	0.709
30.90	0.624	31.07	0.624	31.33	0.623
25.98	0.531	26.26	0.527	26.66	0.528
20.25	0.429	20.55	0.430	21.00	0.432
14.81	0.332	15.05	0.332	15.41	0.329
T = 310.97 K		T = 323.24 K		T = 333.49 K	
35.84	0.984	35.64	0.962	35.11	0.863
35.58	0.893	35.14	0.813	34.18	0.703
34.97	0.790	34.03	0.699	32.31	0.612
33.76	0.698	31.99	0.617	28.48	0.517
31.50	0.615	27.89	0.522	23.22	0.426

27.11	0.523	22.46	0.425	17.36	0.327
21.57	0.429	16.67	0.324		
15.90	0.328				
T = 350.01 K		T = 377.14 K		T = 398.15 K	
34.52	0.770	33.45	0.795	31.90	0.615
33.70	0.663	32.86	0.616	31.80	0.585
32.13	0.584	31.62	0.536	31.70	0.566
28.71	0.496	28.78	0.462	31.60	0.556
23.82	0.408	24.43	0.388	31.29	0.526
18.04	0.318	18.91	0.303	30.80	0.486
				28.37	0.429
				24.48	0.366
T = 410.62 K		T = 423.12 K			
31.14	0.413	29.31	0.340		
31.11	0.431	28.51	0.362		
31.06	0.443	26.63	0.347		
30.96	0.454	23.46	0.303		
30.74	0.453				
30.27	0.445				
29.33	0.424				
27.19	0.385				
23.68	0.328				

[a]Standard temperature uncertainty $u(T)$: 0.02 K; Standard pressure uncertainty $u(p)$: 0.06 MPa; Standard liquid fraction uncertainty u(Liquid fraction): 0.009.

The obtained equilibrium pressures were compared with the literature data published by Sage et al. [17], Reamer et al. [18] and Rijkers et al. [7]. These literature data cover the whole composition range and the temperature range from (245 to 510) K.

As concerns the mixture with x_1=0.4031, the obtained equilibrium pressures were compared with the literature data from Rijkers et al. [7] with methane mole fraction x_1=0.4049 in the temperature range from (303 to 348) K resulting in an AAD of 3.1%. Also, a comparison with the data from Reamer et al. [18] (x_1=0.3943) at temperatures between 310 and 444 K yielded an AAD of 2.4%.

Regarding the mixture with x_1=0.6021, the obtained equilibrium pressures were compared with the data from Sage et al. [17] with methane mole fraction x_1=0.5997 at temperatures between 294 and 394 K, yielding an AAD of 1.0%. Moreover, Reamer et al. [18] have also reported equilibrium pressures for the system methane (1) + n-decane (2) with x_1=0.5820, which yielded an AAD of 5.1% when compared with the data reported in this work at temperatures between 310 and 444 K. This was the highest AAD when comparing the equilibrium pressures obtained in this work with literature data corresponding to a maximum difference of 1.3 MPa. This high deviation could be explained due to the composition difference between the compared mixtures, which is higher than in the other comparisons with literature data.

Finally, concerning the mixture with x_1=0.8496, the equilibrium pressures obtained in this work were compared with literature data from Reamer et al. [18] (x_1=0.8573) at temperatures between

310 and 444 K yielding an AAD of 1.1%. Additionally, the AAD between the obtained values and the literature data from Rijkers et al. [7] for x_1=0.8586 in the temperature range from (320 to 350) K is 0.2%.

A summary of the relative deviations obtained after comparison among the equilibrium pressures reported in the present work and those from literature is plotted in Fig. 10. As it can be observed, both positive and negative deviations with previously reported experimental data [7,17,18] were found. Moreover, all deviations are within ±7%.

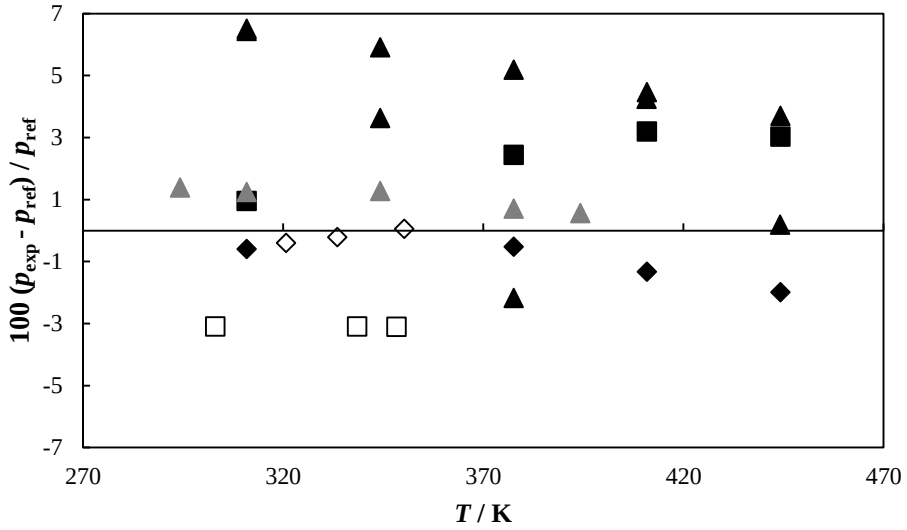

Fig. 10. Relative deviations between the equilibrium pressures obtained in this work and those from literature for the system methane (1) + n-decane (2) with x_1=0.4031 (□), x_1=0.6021 (△) and x_1=0.8496 (◇). Black symbols are comparison with Reamer et al. [18] (x_1=0.3943, x_1=0.5820, x_1=0.8573), empty symbols with Rijkers et al. [7] (x_1=0.4049, x_1=0.8586) and grey symbols with Sage et al. [17] (x_1=0.5997).

The phase envelope obtained through SRK, PR, PC-SAFT and S-BWR, as well as the calculated critical points for the mixtures are depicted together with the experimental data in Figs. 11, 12 and 13 for the three different compositions studied in this work. A quantitative description of the deviations is presented in table 14, where the AAD, bias and maximum deviation are presented. It is worth noting that, due to the poor performance of S-BWR, it was not taken into account in the quantitative comparison of model performance.

Table 14

Absolute average deviation (AAD), bias, and maximum deviation (D_{max}) for the calculated saturation pressure of the binary system methane (1) + n-decane (2) in the whole experimental (p,T,x) range through the different EoS with k_{ij} values from table 3.

	SRK	PR	PC-SAFT
x_1 = 0.4031			
AAD / %	0.9	0.8	4.5
bias / %	-0.4	-0.6	-4.5

D_{max} / %	3.6	3.0	7.4
x_1= 0.6021			
AAD / %	0.9	1.6	2.8
bias / %	-0.4	-1.6	-2.7
D_{max} / %	3.1	4.7	5.0
x_1 = 0.8496			
AAD / %	14	8.7	7.4
bias / %	14	8.7	6.2
D_{max} / %	20	11	10

Taking into account the absolute average deviation (Fig. 14) between experimental and calculated saturation pressures of each model, PR has the lowest AAD for the mixture with x_1=0.4031, SRK for x_1=0.6021 and PC-SAFT for x_1=0.8496. The mixture with x_1=0.8496 presents the highest deviations, especially at low temperatures. Generally, the AAD for the system methane (1) + n-decane (2) with x_1=0.8496 for all the models is much higher than for the two other compositions. We investigated how tuning of k_{ij} can improve the model performance for the mixture with x_1=0.8496. It is possible to get better fitting of the experimental data by lowering the k_{ij} values for SRK, PR and PC-SAFT. As concerns S-BWR, it is impossible to improve its results significantly by tuning its k_{ij}. The tuned k_{ij} values are summarized in table 15, and the phase envelopes obtained for the mixture with x_1=0.8496 by using the new k_{ij}s are also included in Figure 13. It can be observed that the calculated envelopes are improved and that PR and PC-SAFT give closer saturation pressures than SRK. However, it should be pointed out that the new k_{ij}s tend to give smaller phase envelopes and the envelopes calculated by SRK, PR and PC-SAFT for x_1=0.4031 and x_1=0.6021 (not shown here) will give larger deviations than those with the original k_{ij}s. It shows that accurate modeling of phase equilibrium for a highly asymmetric system, even as simple as methane+n-decane, over a wide temperature, pressure and composition range is not an easy task.

Table 15
Tuned methane/n-decane binary interaction parameters, k_{ij}, for the EoSs studied in this work.

	SRK	PR	PC-SAFT
k_{ij}	0.020	0.025	0.010

Moreover the calculated critical temperatures for the systems methane (1) + n-decane (2) with x_1=0.4031 and x_1=0.6021 are higher than the experimental ones, which is in agreement with the fact that the observed saturation points were bubble points. Furthermore, the equilibrium pressures values of the system with x_1=0.8496 identified as bubble points, i.e. from (293.15 to 397.96) K, are in reasonable agreement with the critical point calculated by PC-SAFT whereas critical points given by means of PR and SRK are in disagreement with the experimentally observed bubble and dew points for this last binary mixture.

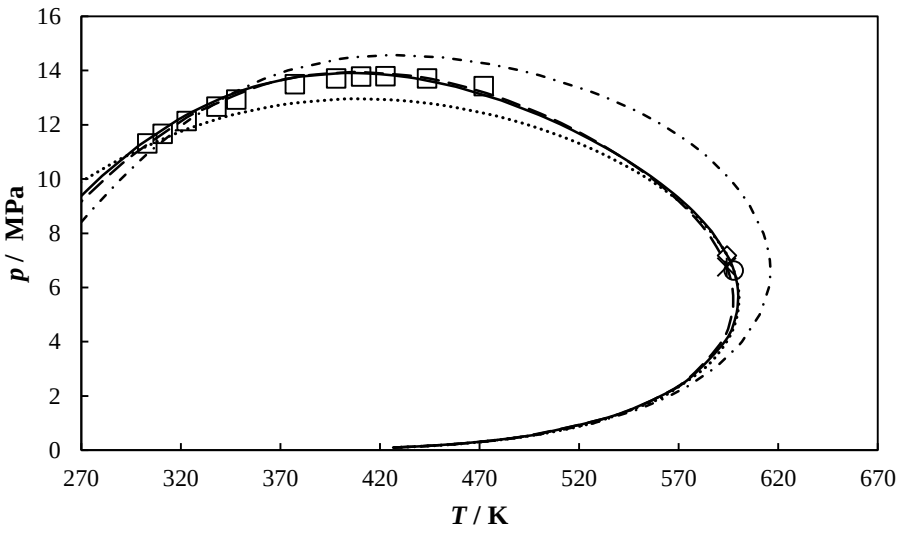

Fig. 11. Experimental values of the equilibrium pressure for the system methane (1) + n-decane (2) with x_1=0.4031 (□). Lines are the results for SRK (—), PR (– –), PC-SAFT (···) and S-BWR (-·-); SRK critical point (○), PR critical point (∗), PC-SAFT critical point (◇) with k_{ij} values from table 3.

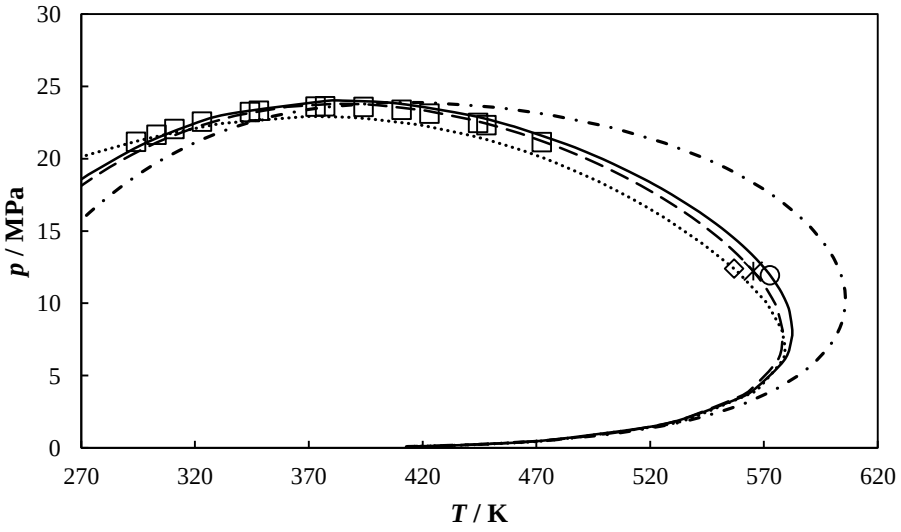

Fig. 12. Experimental values of the equilibrium pressure for the system methane (1) + n-decane (2) with x_1=0.6021 (□). Lines are the results for SRK (—), PR (– –), PC-SAFT (···) and S-BWR (-·-); SRK critical point (○), PR critical point (∗), PC-SAFT critical point (◇) with k_{ij} values from table 3.

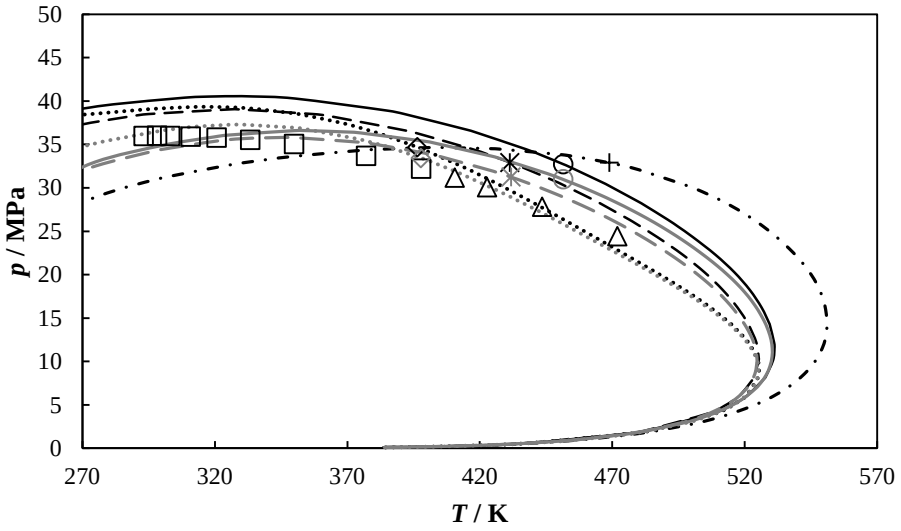

Fig. 13. Experimental values of the equilibrium pressure for the system methane (1) + n-decane (2) with x_1=0.8496: bubble points (□), dew points (△). Lines are the results for SRK (—), PR (– –), PC-SAFT (···) and S-BWR (-·-); The black lines indicate results with k_{ij} values from table 3, whereas the grey lines indicate results with the tuned k_{ij} from table 15. SRK critical point (○), PR critical point (∗), PC-SAFT critical point (◇), S-BWR critical point (+)

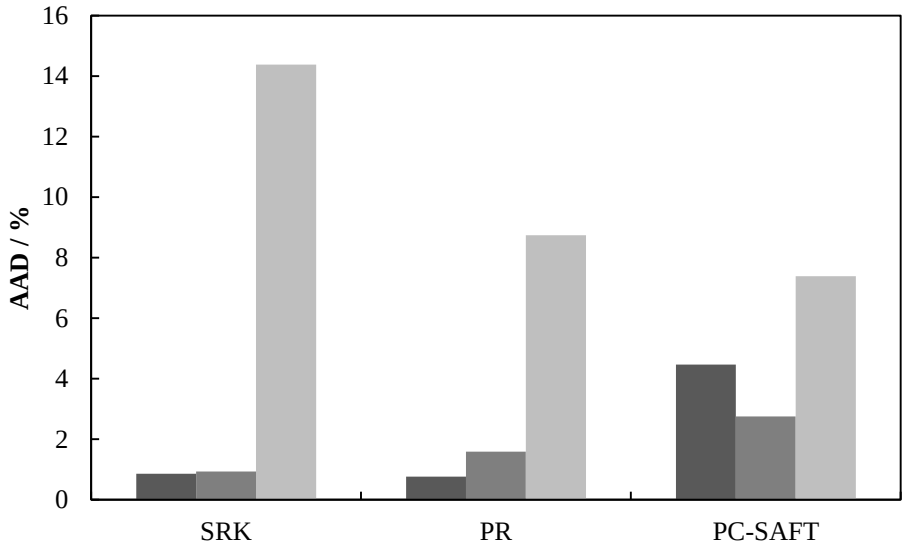

Fig. 14. Absolute average deviation (AAD) for the calculated saturation pressures for the system methane (1) + n-decane (2) by different models with the k_{ij} values from table 3. x_1=0.4031 (■), x_1=0.6021 (■) and x_1=0.8496 (■).

4. Conclusions

We have reported data on density for the binary system methane + n-decane which extends the data previously reported for this system to lower and higher temperatures, as well as to higher pressures. Among the SRK, PR, PC-SAFT and S-BWR EoSs, all using k_{ij}s previously regressed from binary VLE data, PC-SAFT gives the best description for the measured density, yielding an AAD of 0.9

%. Excess volumes obtained from density measurements are negative in the whole studied (p,T,x) range, becoming more negative as the pressure decreases or the temperature increases. SRK, PR and PC-SAFT EoSs give reasonable description for the measured excess volumes whereas the values calculated by S-BWR are inaccurate.

As regards the density derived properties, the expected dependences were obtained for the isothermal compressibility, i.e., increasing with methane mole fraction and temperature, and decreasing with pressure. Moreover calculations of this property through the GERG-2008 EoS yielded an AAD of 5.3%. As for the thermal expansion coefficient, a crossover region among the isotherms of the α_p vs. p plot was found in all the studied binary mixtures.

As concerns the reported phase equilibrium data of the binary system methane (1) + n-decane (2), they are in agreement within 6.5% with previously reported data. Bubble points were found in the whole range of studied temperatures for the mixtures with x_1=0.4031 and x_1=0.6021, whereas for the mixture with x_1=0.8496 bubble points were obtained in the temperature range from 293.15 K to 397.96 K and dew points from 410.66 K to 472.12 K. The measurements of the liquid fraction (V_{liquid}/V_{total}) upon expansion below the saturation pressure were reported and used to determine whether the phase transition was a bubble or a dew point for the last mixture.

The saturation pressures calculated by SRK, PR and PC-SAFT are acceptable for the mixtures with lower methane mole fractions, whereas they become poor when the methane mole fraction in the mixture is high (x_1=0.8496). This highlights the challenge of predicting phase envelopes of highly asymmetric systems with k_{ij}s regressed from binary VLE. Such systems, characterized by high methane content and a significant amount of heavy components, are typical of gas condensates and volatile oils in reservoir fluids. However, by tuning the k_{ij} values it is possible to get a better representation of this last mixture through SRK, PR and PC-SAFT. Moreover, according to the experimental observations for the mixture with x_1=0.8496, the most accurate prediction of the critical temperature is given by PC-SAFT.

Acknowledgements

This work has been carried out under the NextOil project sponsored by Innovation Fund Denmark, DONG E&P and Maersk Oil. Authors acknowledge also Farhad Varzandeh for his help in the calculations.

References

[1] A. Shadravan, M. Amani, HPHT 101-What petroleum engineers and geoscientists should know about high pressure high temperature wells environment, Energy Sci. Technol., 4 (2012) 36-60.

[2] Delivering success in HP/HT reservoirs through experience, innovation and reliable technologies, in: High pressure/High temperature (HP/HT), H07779 01/11, Halliburton, 2011.

[3] M.J. Cebola, G. Saville, W.A. Wakeham, Vapor–liquid equilibrium in the ternary system methane-n-hexane-n-tetradecane, Fluid Phase Equilib., 150–151 (1998) 703-711.

[4] F. Audonnet, A.A.H. Pádua, Viscosity and density of mixtures of methane and n-decane from 298 to 393 K and up to 75 MPa, Fluid Phase Equilib., 216 (2004) 235-244.

[5] P. Ungerer, B. Faissat, C. Leibovici, H. Zhou, E. Behar, G. Moracchini, J.P. Courcy, High pressure-high temperature reservoir fluids: investigation of synthetic condensate gases containing a solid hydrocarbon, Fluid Phase Equilib., 111 (1995) 287-311.

[6] M.P.W.M. Rijkers, V.B. Maduro, C.J. Peters, J. de Swaan Arons, Measurements on the phase behavior of binary mixtures for modeling the condensation behavior of natural gas: Part II. The system methane + dodecane, Fluid Phase Equilib., 72 (1992) 309-324.
[7] M.P.W.M. Rijkers, M. Malais, C.J. Peters, J. de Swaan Arons, Measurements on the phase behavior of binary hydrocarbon mixtures for modelling the condensation behavior of natural gas: Part I. The system methane + decane, Fluid Phase Equilib., 71 (1992) 143-168.
[8] J.M. Shaw, T.W. de Loos, J. de Swaan Arons, Prediction of unusual retrograde condensation in model reservoir fluids, Fluid Phase Equilib., 84 (1993) 251-266.
[9] J.A. Amorim, O. Chiavone-Filho, M.L.L. Paredes, K. Rajagopal, High-pressure density measurements for the binary system cyclohexane + n-hexadecane in the temperature range of (318.15 to 413.15) K, J. Chem. Eng. Data, 52 (2007) 613-618.
[10] T. Regueira, W. Yan, E.H. Stenby, Densities of the binary systems n-hexane + n-decane and n-hexane + n-hexadecane up to 60 MPa and 463 K, J. Chem. Eng. Data, 60 (2015) 3631-3645.
[11] X. Canet, A. Baylaucq, C. Boned, High-pressure (up to 140 MPa) dynamic viscosity of the methane+decane system, Int. J. Thermophys., 23 (2002) 1469-1486.
[12] G. Soave, Equilibrium constants from a modified Redlich-Kwong equation of state, Chem. Eng. Sci., 27 (1972) 1197-1203.
[13] D.-Y. Peng, D.B. Robinson, A new two-constant equation of state, Ind. Eng. Chem. Fundam., 15 (1976) 59-64.
[14] J. Gross, G. Sadowski, Perturbed-Chain SAFT: An equation of state based on a perturbation theory for chain molecules, Ind. Eng. Chem. Res., 40 (2001) 1244-1260.
[15] G.S. Soave, An effective modification of the Benedict–Webb–Rubin equation of state, Fluid Phase Equilib., 164 (1999) 157-172.
[16] A. Danesh, PVT and phase behaviour of petroleum reservoir fluids, Elsevier, Amsterdam, 1998.
[17] B.H. Sage, H.M. Lavender, W.N. Lacey, Phase equilibria in hydrocarbon systems methane–decane system, Ind. Eng. Chem., 32 (1940) 743-747.
[18] H.H. Reamer, R.H. Olds, B.H. Sage, W.N. Lacey, Phase equilibria in hydrocarbon systems, Ind. Eng. Chem., 34 (1942) 1526-1531.
[19] W. Yan, F. Varzandeh, E.H. Stenby, PVT modeling of reservoir fluids using PC-SAFT EoS and Soave-BWR EoS, Fluid Phase Equilib., 386 (2015) 96-124.
[20] M.J.P. Comuñas, J.-P. Bazile, A. Baylaucq, C. Boned, Density of diethyl adipate using a new vibrating tube densimeter from (293.15 to 403.15) K and up to 140 MPa. Calibration and measurements, J. Chem. Eng. Data, 53 (2008) 986-994.
[21] W. Wagner, A. Pruß, The IAPWS formulation 1995 for the thermodynamic properties of ordinary water substance for general and scientific use, J. Phys. Chem. Ref. Data, 31 (2002) 387-535.
[22] E.W. Lemmon, M.L. Huber, Thermodynamic properties of n-dodecane, Energy Fuels, 18 (2004) 960-967.
[23] J.J. Segovia, O. Fandiño, E.R. López, L. Lugo, M. Carmen Martín, J. Fernández, Automated densimetric system: Measurements and uncertainties for compressed fluids, J. Chem. Thermodyn., 41 (2009) 632-638.
[24] N. von Solms, M.L. Michelsen, G.M. Kontogeorgis, Computational and physical performance of a modified PC-SAFT Equation of State for highly asymmetric and associating mixtures, Ind. Eng. Chem. Res., 42 (2003) 1098-1105.
[25] Design Institute for Physical Property Research Database DIPPR Project 801, in, Design Institute for Physical Property Research / AIChE, 2015.

[26] D. Ambrose, C. Tsonopoulos, Vapor-liquid critical properties of elements and compounds. 2. Normal alkanes, J. Chem. Eng. Data, 40 (1995) 531-546.
[27] Calculated by project staff at Brigham Young University using either internal or published prediction methods
[28] A.J. Perkins, Predicted by project staff at The Pennsylvania State University using either published or internal methods
[29] E.W. Lemmon, R. Span, Short fundamental equations of state for 20 industrial fluids, J. Chem. Eng. Data, 51 (2006) 785-850.
[30] I. Cibulka, L. Hnědkovský, Liquid densities at elevated pressures of n-alkanes from C5 to C16: A critical evaluation of experimental data, J. Chem. Eng. Data, 41 (1996) 657-668.
[31] U. Setzmann, W. Wagner, A new equation of state and tables of thermodynamic properties for methane covering the range from the melting line to 625 K at pressures up to 100 MPa, J. Phys. Chem. Ref. Data, 20 (1991) 1061-1155.
[32] G. Katzenski, G.M. Schneider, Excess volumes of liquid n-alkane binaries from 10 to 200 MPa at 298.15 K, J. Chem. Thermodyn., 14 (1982) 801-802.
[33] G.M. Schneider, Fluid mixtures at high pressures, in: Pure Appl. Chem., 1983, pp. 479.
[34] L. Lepori, P. Gianni, E. Matteoli, The effect of the molecular size and shape on the volume behavior of binary liquid mixtures. Branched and cyclic alkanes in heptane at 298.15 K, J. Solution Chem., 42 (2013) 1263-1304.
[35] D. Apam-Martínez, A. Trejo, Excess heat capacities and excess volumes of n-alkane mixtures, J. Chem. Soc., Faraday Trans. 1, 84 (1988) 4073-4086.
[36] A. Trejo-Rodríguez, D. Patterson, Prediction of excess volumes of n-alkane mixtures through the corresponding-states principle, J. Chem. Soc., Faraday Trans. 2, 81 (1985) 177-187.
[37] O. Kunz, W. Wagner, The GERG-2008 wide-range Equation of State for natural gases and other mixtures: An expansion of GERG-2004, J. Chem. Eng. Data, 57 (2012) 3032-3091.
[38] J. Troncoso, P. Navia, L. Romaní, D. Bessieres, T. Lafitte, On the isobaric thermal expansivity of liquids, J. Chem. Phys., 134 (2011) 094502.